

1.13 NOWCASTING PROBLEM IN A SUBTROPICAL AREA WITH COMPLEX TERRAIN: LESSON LEARNED FROM A FLASH FLOOD CASE

Ben Jong-Dao Jou*

Department of Atmospheric Sciences

National Taiwan University

Taipei, Taiwan

1. Introduction

In the afternoon of 21 June 1991, a complex thunderstorm system developed over the metropolitan area of Taipei city and brought heavy rainfall and flash flood. This event occurred without any timing warning and caused large property damage. By examining the mesonet and the Doppler radar data, it can be shown that the sea breeze, the upslope wind, the outflow boundary induced by the precipitation, and the direction of the prevailing wind all contributed to the formation of this flash flood event. The heated terrain initiated the cumulus cloud development and the sea breeze provided excess water vapor for further cloud development into a severe thunderstorm system. On the other hand, the trajectory of the storm, presumably followed the direction of prevailing mean wind, was modified by outflows caused by the heavy precipitation and the sloping terrain. The interaction between the environment and the mesoscale processes makes the forecast a very difficult situation. In this study, the movement and propagation of the thunderstorm system is described by using the Doppler radar located at CKS International Airport in northern Taiwan. The possible mechanisms related to the interactions among the environmental winds, the sea breeze circulation, the mountain slope, and the storm-generated outflows are discussed. In the concluding section, the need for a nowcasting system in a subtropical island with complex terrain is discussed.

2. Storm Evolution and Propagation

A sequence of 3 km CAPPI radar reflectivity maps from CKS Doppler radar was analyzed (figure not shown). It can be seen that the first echo of the storm system was observed 30 km southeast of the Taipei basin over the mountainous area at around 1100LST. The early development of the echoes was oriented in a NE-SW direction parallel to the mountain range and near the mountain peak. The echoes gradually evolved into a linear feature and became a multi-cellular thunderstorm system (Fig.1).

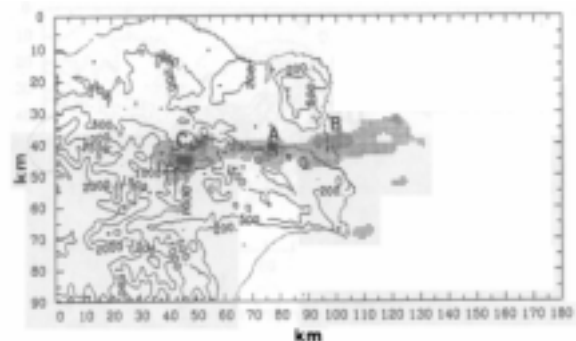


Fig.1 Radar reflectivity map at 3 km height on 1335 LST 21 June 1991. The beginning shading is 30 dBZ. The dark shading represents radar echo larger than 45 dBZ. The thin lines indicate the terrain contours (200m, 500m, 1000m, and 1500m, respectively). The three major convective storms discussed in the text are indicated by A, B, and C.

The storm system intensified rapidly and showed an explosive development as it reached the foothills southeast of the Taipei Basin (1330LST). The major heavy rain area (defined by the equivalent reflectivity factor $Z_e \geq 40$ dBZ, corresponding to a rainfall rate approximately 15 mm/h) became an elongated compound feature at 1400LST. The storm system

* Corresponding author address: Prof. Ben Jong-Dao Jou, National Taiwan University, Department of Atmospheric Sciences, Taipei, Taiwan, 106; e-mail: jou@webmail.as.ntu.edu.tw

reached its mature stage (defined by the period when the precipitation area with $Z_e \geq 45 \text{ dBZ}$ reached its maximum value) in the Taipei basin at around 1500LST. The storm possessed strong reflectivity intensity during the period of 1500-1600LST and dissipated afterwards.

There are some interesting phenomena associated with the evolution of the storm system. First, the storm at its mature stage delivered heavy rain over an area very similar to the geographic configuration of Taipei basin. It occupied an area about 40 km long and 20 km wide. The heavy rain period lasted about 3 hours (from 1300-1600LST) and the accumulated rainfall was more than 140 mm. If estimated by the rainfall rate of 15mm/h during its mature stage, the total water deposited each hour into this area is twelve million metric tons. It is no surprise that even the Presidential Palace at the center of the Taipei city was flooded that afternoon. Second, the storm system developed into a complex mesoscale feature after it reached the mature stage. The convective precipitation area extended northeastward along the mean low-to-middle tropospheric wind direction and dissipated rapidly after moved into the ocean. Third, the storm intensified rapidly after it reached the foothills at about 1400 LST and it was about the time the sea breeze front marching from west coast to arrive the foothill of the Snow mountain range on the east of the basin. Finally, there was a secondly development of the storm system in the mountainous areas in late afternoon and prolonged the lifetime of the storm significantly.

Fig.2 shows the time evolution maximum radar reflectivity cross section passing Taipei basin in a NW-SE orientation. This cross section can be treated as the time evolution of maximum reflectivity of a storm initiated near the mountain peak. The movement of the storm system in a whole was westward, however, when examined in detail, the reflectivity data showed the individual major precipitation centers, defined by the areas with $Z_e \geq 40 \text{ dBZ}$, moved differently. Three major precipitation centers were identified during this period and each of them presented a quite different trajectory. To the south of Taipei, the storm C initiated at a higher terrain and moved northeastward downslope to the basin with a speed of 6.3m/s. To the east of Taipei, two major storms (A and B) moved westward also downslope to the basin. The speed of

these two storms was much slower than C, with 3.4 and 2.3 m/s, respectively. The speed of the storm was even slower (near stationary) while they were at the Taipei basin. It also noticed that the storm A moved northwestward in the sloping area and then moved southwestward after it was in the basin. This direction change occurred over the foothills southeast of the Taipei basin, indicating a subtle relation between the storm propagation and the complex terrain surrounding the Taipei city.

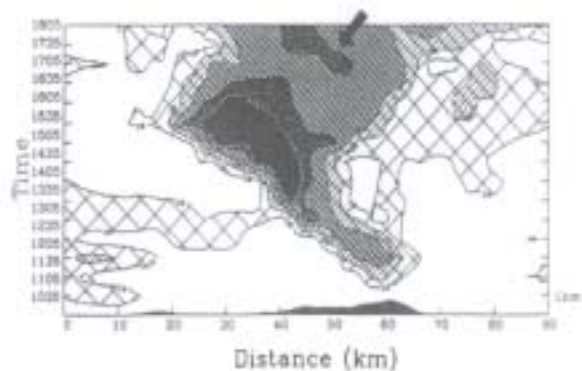


Fig.2 Time evolution of maximum radar reflectivity in cross section passing the Taipei basin in northwest-southeast (70-79km) direction. The beginning contour is 10 dBZ and increase by 10dBZ. The terrain feature is shown at the bottom of the figure.

It was noted that the storm intensified significantly over the foothill and reached its mature stage in the basin. According to Taipei surface station observations (Fig.3), the storm brought 100mm rainfall within an hour from 1453-1553 LST, and had its maximum 10-minute maximum rainfall rate (23 mm/10 min) from 1515 to 1525 LST. The height-time indicator (HTI) of radar reflectivity over the Taipei station showed strong echoes ($>40 \text{ dBZ}$) extended from surface to 7 km height and occurred at about the same time period when the surface rain gauge station measured heavy rain rates. It is also noted that while the storm was passing by the station, surface temperature at the station dropped from 30C to 25.5C, the surface pressure increased from 999.8 hPa to 1001.8 hPa, and the surface wind changed from westerly to easterly abruptly. All these observations indicate the existence of a strong cold pool of air and the appearance of this cold pool air was associated with the heavy precipitation of the storm. The cold pool air persisted with the heavy rain and had a character of

higher pressure, lower temperature, and sudden change of winds. Similar phenomena were observed by Charba (1974) in squall line gust fronts, by Goff (1976) in thunderstorm outflows, and by Frankhauser (1976) in hailstorms. With high temporal and spatial resolution of Doppler radar data, Wakimoto (1982) studied the life cycle of thunderstorm outflow phenomena. It was shown that the formation of the cold pool air with sudden wind change is caused by evaporation of raindrops and convective downdrafts embedded within the storm system. The leading edge of this cold pool air forms the gust front that commonly produces significant convergence and is favorable for triggering new storms.

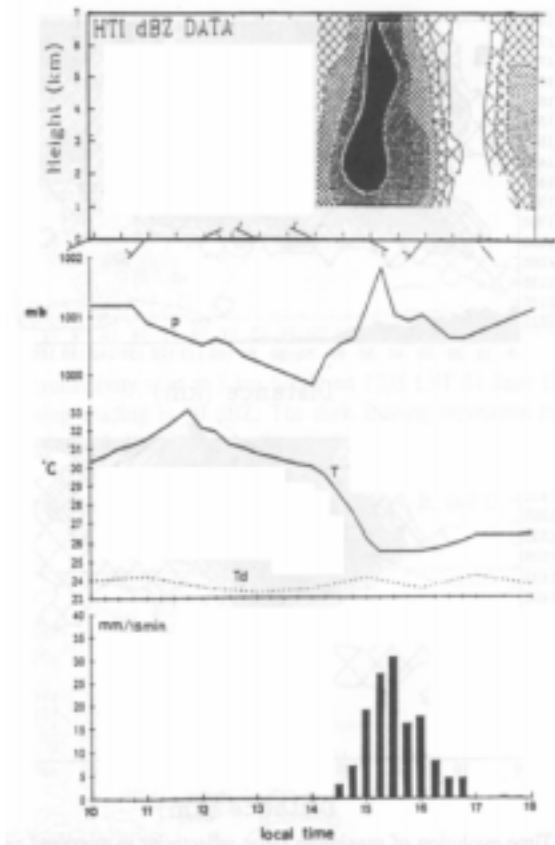


Fig.3 Surface observations of winds, pressure, temperature, dew point, and rainfall intensity at Taipei station from 1000 to 1800 LST 21 June 1991. The rainfall data is at 15-minute intervals and others are hourly data. On the top of the figure, the corresponding height-time indicator(HTI) of radar reflectivity over Taipei station is also given.

3. Low-Level Flow Evolution Inferred from Doppler Velocity

Wilson and Schreiber (1986) had demonstrated the importance of boundary layer convergence lines on storm initiation east of Colorado Rocky Mountains by using Doppler radar data. Fig.4 shows a sequence of vertical cross sections of horizontal winds perpendicular to the storm system derived both from the reflectivity factor and also the radial velocity. Since the radial velocity only sampled a partial component of the true total velocity, the derived wind field (projected on the cross section we chose) could only be interpreted in a qualitative manner. The heavy-shading region is flow from right (called easterly wind for convenience) with magnitude less than 5 m/s, while the lighter-shading region is flow from left (called westerly wind) with magnitude less than 5 m/s, respectively. The following discussion will be focused only on the low level flows due to the limitation of the derived wind field. In the early development stage, the low level winds revealed several different mesoscale features during this relatively undisturbed period. Weak westerly winds prevailed in most areas in northern Taiwan in the late morning hours. Over the mountainous region, on the other hand, weak easterly winds presented in the lower troposphere. The shallow convection in the mountain was embedded in the low level easterly regime and located at a position some distance away from the convergence line formed by the low-level westerly and easterly flows. In Fig.4, the convergence line was enhanced by the white color zone.

Over the western slope and the Taipei basin, stronger westerly winds (>5 m/s, heavier shaded) were observed by the radar in the lowest 1.5 km after 1200 LST. This stronger westerly winds occurred in the atmospheric boundary layer (ABL) and progressed eastward in the middle of the day suggesting the existence of the thermally-driven sea breeze circulation. The leading edge of this stronger westerly wind reached the foothill at around 1300 LST and was also detected by the surface stations around the Taipei basin (figure not shown). The development of the upslope flow along the western slope of the mountain was also observed by the Doppler radar. The leading edge of the westerly wind within the ABL moved upslope to the higher mountain at 1300LST. The penetration of the upslope winds into the higher terrain provided a possible triggering mechanism for mountainous convection development.

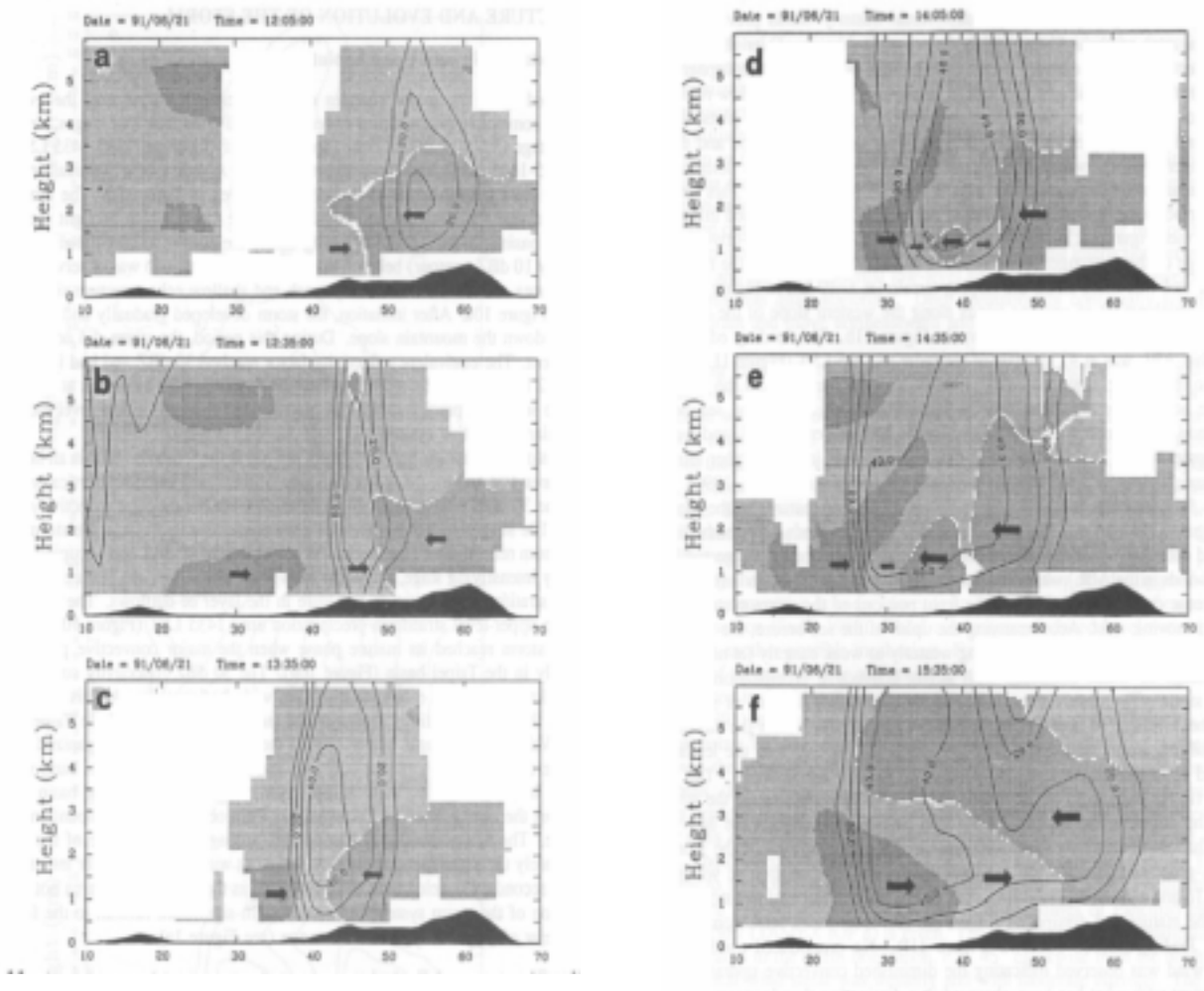


Fig.4 A sequence of horizontal winds perpendicular to storm orientation, derived from the CAA Doppler radar's radial velocity data at selected time on 21 June 1991. The cross sections are selected to pass the Taipei basin in northwest-southeast direction. The heavy-shading represents flow from the east and the lighter-shading represents flow from the west with speed less than 5 m s^{-1} . Within the westerly flow regime, the heavier-shading represents flow from the west but with speed greater than 5 m s^{-1} . The mean terrain feature is shown at bottom of the figure.

The flow structure revealed a quite different flow regime in the rapid intensifying stage. The upslope flow and sea breeze were both disturbed by the intensified storm system. The leading edge of the sea breeze was lifted to a much higher altitude within the storm indicating the existence of the intensive convective updraft at the front position (moving westward) of the storm. Accompanying the uplift of the sea breeze, the wind in ABL over the foothill abruptly changed from stronger westerly to weak easterly. This abrupt change of wind direction coincided with the appearance of strong precipitation echoes associated with the storm. A pronounced divergent flow pattern was observed at this period indicating the existence of

convective downdraft. In summary, the intensifying storm system had its major updraft on the leading edge and its major downdraft embedded within the storm. The updraft seemed to tilt eastward. The downdraft produced pronounced outflows underneath the heavy precipitation area. Enhanced local convergence in ABL at the front portion of the storm was observed and possibly induced by the storm-generated cold pool outflow and the inland-penetration of the sea breeze.

In the dissipating stage, the low-level flows were dominated by the precipitation induced outflows. No pronounced uplift of the low level westerly wind was observed indicating the diminished convective updrafts. These features are consistent with what has been

observed in a dissipating thunderstorm.

4. Concluding Remarks

In this study, a mountain-originated complex thunderstorm system in northern Taiwan was investigated. The evolution and propagation of the storm system was studied by a C-band Doppler radar. The interactions among the sea breeze circulation, the mountain induced sloping winds, and the precipitation induced outflows were discussed. To summarize, the cumulus convection seemed to be triggered by thermal forcing on the mountain top. In the early developing stage, the storm propagation was mainly controlled by the so-called translation process, i.e., propagated along the prevailing southwesterly flows and gradually formed into a NE-SW line. The trajectory of each major convective storm was modulated by the sloping terrain. The modification became effective while significant precipitation occurred. The outflows interacted with the mountain induced upslope winds to provide the necessary lifting for new convections to form on the west side of the old storm. Storm propagation at this stage was a result of combined effect of forced mechanism and the auto-propagation mechanism as suggested in Cotton and Anthes (1989). The storm moved into the basin at its mature stage. Enhanced convergence induced by the inland sea breeze and the storm-generated outflows and abundance of low-level moisture associated with the sea breeze circulation provided the conditions for pronounced storm intensification and heavy rainfall. The storm was almost stationary in the basin area. Sloping terrain has no role at this stage. The interaction between the storm generated outflows and the low-level environmental winds favored new cells to form in the southwest quadrant of the system. A combination of the translation process by the mean wind (toward northeast) and the auto-propagation process (toward southwest) resulted in a near stationary storm propagation. New storm cells merged with the old cells along the same trajectory, hence, brought the heavy rain to the same location in a relatively short period of time.

From the above discussion, we have seen that the complex terrain in the northern Taiwan plays a subtle role in controlling the organization, propagation, and development of the severe multi-cellular

thunderstorm systems in the area. We have demonstrated, in this case study, that the importance of Doppler radar and mesonet in revealing the important mesoscale features and also the mesoscale processes associated with the formation and the propagation of this complex storm system. It is not clear, however, which process(es) is (are) more important under different environmental conditions. Possibly due to the fast growth of the metropolitan area of Taipei city and possibly due to the global warming, the damages caused by these severe rainstorms in the great area of Taipei (an area of approximately 3,000 km² with a population of 6 million) has been increased dramatically in the last 10 years. In order to improve the forecast capability and to mitigate the damages caused by these short-term localized severe rainstorms, a very short term nowcasting system is needed. To establish a workable forecast system, a comprehensive observational and numerical simulation study is needed in order to get a better understanding of all these complicated mesoscale processes in complex terrain environment of northern Taiwan.

Acknowledgements This research has been supported partially by the National Science Council of the Republic of China under Grants NSC 93-2111-M-002-015-AP2 and NSC93-2625-Z-002-008.

References

- Charba, J., 1974: Application of gravity current model to analysis of squall line gust front. *Mon. Wea. Rev.*, 102, 140-156.
- Cotton, W. R., and R. A. Anthes, 1989: *Storm and Cloud Dynamics*. Academic Press, San Diego, 883pp.
- Frankhauser, J. C., 1976: Structure of an evolving hailstorm. Part II: Thermodynamic structure and airflow in the near environment. *Mon. Wea. Rev.*, 104, 576-587.
- Goff, R. C., 1976: Vertical structure of thunderstorm outflow. *Mon. Wea. Rev.*, 104, 1429-1440.
- Wakimoto, R. M., 1982: The life cycle of thunderstorm gust fronts as viewed with Doppler radar and rawinsonde data. *Mon. Wea. Rev.*, 110, 1050-1082.
- Wilson, J. W., and W. E. Schreiber, 1986: Initiation of convective storms at radar observed boundary layer convergence lines. *Mon. Wea. Rev.*, 114, 2516-2536.